Monoclonal Antibody Characterization of Two Distant Sites Required for Function of the Central Cell-binding Domain of Fibronectin in Cell Adhesion, Cell Migration, and Matrix Assembly

Toshihiko Nagai,*‡§ Naomi Yamakawa,*‡ Shin-ichi Aota,‡ Susan S. Yamada,‡ Steven K. Akiyama,*‡ Kenneth Olden,*‡ and Kenneth M. Yamada‡

*Howard University Cancer Center, Washington DC 20060; ‡Laboratory of Developmental Biology, National Institute of Dental Research, National Institutes of Health; and §Laboratory of Molecular Biology, National Cancer Institute, National Institutes of Health, Bethesda, Maryland 20892

Abstract. Site-directed mutagenesis studies have suggested that additional peptide information in the central cell-binding domain of fibronectin besides the minimal Arg-Gly-Asp (RGD) sequence is required for its full adhesive activity. The nature of this second, synergistic site was analyzed further by protein chemical and immunological approaches using biological assays for adhesion, migration, and matrix assembly. Fragments derived from the cell-binding domain were coupled covalently to plates, and their specific molar activities in mediating BHK cell spreading were compared with that of intact fibronectin. A 37-kD fragment purified from chymotryptic digests of human plasma fibronectin had essentially the same specific molar activity as intact fibronectin. In contrast, other fragments such as an 11.5-kD fragment lacking NH_2-terminal sequences of the 37-kD fragment had only poor spreading activity on a molar basis. Furthermore, in competitive inhibition assays of fibronectin-mediated cell spreading, the 37-kD fragment was ~325-fold more active than the GRGDS synthetic peptide on a molar basis. mAbs were produced using the 37-kD protein as an immunogen and their epitopes were characterized. Two separate mAbs, one binding close to the RGD site and the other to a site ~15 kD distant from the RGD site, individually inhibited BHK cell spreading on fibronectin by >90%. In contrast, an antibody that bound between these two sites had minimal inhibitory activity. The antibodies found to be inhibitory in cell spreading assays for BHK cells also inhibited both fibronectin-mediated cell spreading and migration of human HT-1080 cells, functions which were also dependent on function of the $\alpha_5\beta_1$ integrin (fibronectin receptor). Assembly of endogenously synthesized fibronectin into an extracellular matrix was not significantly inhibited by most of the anti-37-kD mAbs, but was strongly inhibited only by the antibodies binding close to the RGD site or the putative synergy site. These results indicate that a second site distant from the RGD site on fibronectin is crucial for its full biological activity in diverse functions dependent on the $\alpha_5\beta_1$ fibronectin receptor. This site is mapped by mAbs closer to the RGD site than previously expected.

CELLULAR adhesion to specific extracellular matrix components is required for a variety of biological events including cell proliferation, embryonic development, wound healing, and disease pathogenesis. The adhesive glycoprotein fibronectin has been an especially important model system for deriving insights into the mechanisms of cell adhesion and migration (8, 9, 23, 36). Fibronectin is a multifunctional glycoprotein with multiple binding activities including those for heparin, collagen, fibrin, and cell surface receptors. These binding activities are contained in distinct, protease-resistant domains. The best characterized cell-binding domain of fibronectin occupies its central region. This central cell-binding domain of fibronectin mediates cell adhesion with a wide variety of cell types (1, 45, 46) through a (Gly)-Arg-Gly-Asp-(Ser) sequence. For example, synthetic peptides containing this sequence block fibronectin-mediated adhesion and binding to cell surface receptors (18, 39, 40, 54). Moreover, direct deletion of the Arg-Gly-Asp (RGD) sequence by site-directed mutagenesis causes a loss of most cell adhesion activity (38).

Although the Arg-Gly-Asp sequence is clearly of great importance as a cell adhesive signal, several major questions remain. In vitro mutagenesis and analysis of bacterially expressed fibronectin fusion proteins indicates that a second

Toshihiko Nagai's present address is Science University of Tokyo, Faculty of Pharmaceutical Sciences, Department of Patho-Physiology, Ichigaya Funagawara-machi, Shinjuku-ku, Tokyo 162, Japan.

Correspondence may be addressed to Dr. Kenneth Yamada, Building 30, Room 414, National Institutes of Health, Bethesda, MD 20892.

major region of the protein is required for adhesive function (4, 38). Studies comparing the biological activities of large and small fibronectin fusion fragments and synthetic peptides derived from fibronectin also indicate that most biological activity is lost when short fibronectin fragments and peptides are assayed even when the RGD sequence is retained (2, 49). Furthermore, the RGD sequence has been found in several adhesive proteins that have distinct functions and specificities and is also found in nonadhesive proteins (39, 45, 52). Consequently, further dissection of the molecular mechanisms of action of fibronectin is required to elucidate how a single molecule can mediate different types of adhesion in different cell types, how the widely distributed RGD peptide sequence can be used as part of specific receptor recognition systems, and how specific sequences in the molecule are used in the more complex processes of cell migration and organization of fibronectin into a three-dimensional fibrillar extracellular matrix (4, 8, 23, 33, 36, 53).

Our original finding of a putative synergistic site (38) that might provide binding affinity and specificity to the fibronectin RGD site has been clouded by several major uncertainties. Because the synergy site was identified using only amino-terminal deletion analysis, the final fusion proteins might have had an incorrect conformation in the region of the RGD recognition site due to the lack of a correct amino-terminal sequence, thus, artifactually producing losses of activity (see also ref. 27). Furthermore, no information was available on which fibronectin receptor(s) could interact with the synergy site and which types of processes involving fibronectin require this "synergy" region, e.g., whether more complex functions such as cell migration or fibronectin matrix assembly require this site. Since the publication of the work of Obara et al. (38), it has been reported that matrix assembly may require both the $\alpha_5\beta_1$ fibronectin receptor and another, unidentified β_1 integrin (13).

A relatively direct, independent approach to answering these questions is the development of specific mAbs that can inhibit fibronectin function. If they can be mapped to different points along the molecule, a series of inhibitory and noninhibitory mAbs can provide insights into which sites are important for function in the form of an independent test of the existence of a second synergy site. They can also provide tests of the role of this site in different biological processes.

In this study, we have characterized a "synergy" region in the central cell-binding domain that is distinct from the RGD site. Our approach has been to isolate and characterize the shortest fully active fragment of fibronectin generated by proteolysis. This protein fragment was then used as an immunogen to obtain mAbs clustered along this key region of fibronectin. These mAbs have then been used in the immunological mapping of sites in fibronectin that are critical for cell spreading and migration, as well as for assembly of a fibrillar fibronectin matrix.

Materials and Methods

Purification of Fibronectin and Fragments

Fibronectin was purified from fresh-frozen citrated human plasma (National Institutes of Health Blood Bank, Bethesda, MD) by gelatin-Sepharose affinity chromatography and citric acid elution (35). The 37-kD fragment was generated by digesting 130 mg fibronectin in 90 ml 0.15 M NaCl, 10 mM Tris-HCl, 0.02% sodium azide, pH 7.4, at 37°C for 20 h with 1.3 mg chymotrypsin (Worthington Biochemicals, Freehold, NJ). The digestion was terminated by adding PMSF to a final concentration of 1 mM. After dialysis against 50 mM Tris-HCl, pH 7.4, the crude digest was applied to a 27-ml bed volume gelatin-Sepharose affinity column. The flow-through fractions were immediately applied to a 44-ml bed volume heparin-Sepharose affinity column. Both affinity columns had been pre-equilibrated with 50 mM Tris-HCl, pH 7.4. The flow-through fractions from the heparin-Sepharose column were pooled and dialyzed against 3 mM sodium phosphate, 0.02% sodium azide, pH 5.8, and applied to a preparative Mitsui Toatsu HCA hydroxyapatite HPLC column (Rainin, Woburn, MA). The column was eluted with a linear gradient of 3 to 120 mM sodium phosphate, pH 5.8, using an FPLC system (Pharmacia LKB Biotechnology, Piscataway, NJ). The material eluting between 95 and 115 mM sodium phosphate was pooled, dialyzed against 1 mM sodium phosphate, pH 6.8, and concentrated by applying to a 2-ml Bio-gel HTP hydroxyapatite column (BioRad Laboratories, Richmond, CA), eluting with 200 mM sodium phosphate, pH 6.8. The eluted material was further concentrated using a Centricon-10 microconcentrator (Amicon Corp., Danvers, MA), and applied to a Superose 12 column (Pharmacia LKB) and eluted with PBS+. Column fractions containing protein as judged by absorbance at 280 nm were analyzed by gel electrophoresis and Western blotting using mAb 333, which binds to fibronectin near the RGD site (2).

The 11.5-kD cell-binding fibronectin fragment was prepared as described using a mAb 333 affinity column (2). Gly-Arg-Gly-Asp-Ser (GRGDS) synthetic peptide was custom synthesized by Immuno-Dynamics, Inc. (La Jolla, CA) and was further purified by reversed phase HPLC and Dowex chromatography before use.

NH_2-terminal and COOH-terminal Amino Acid Sequencing

Purified 37-kD fragment was precipitated with ethanol, washed several times with absolute ethanol, dried by SpeedVac (Savant Instruments, Inc., Hicksville, NY), redissolved in 50% acetic acid, and analyzed by automated gas phase sequencing (Applied Biosystems, Foster City, CA). This amino acid sequence analysis was performed in the Protein Analysis Laboratory of the Cancer Center of Wake Forest University supported in part by NIH grants CA-12197, RR-04869, and a grant from the North Carolina Biotechnology Center. To identify COOH-terminal amino acids, 1.5 nmol of purified 37-kD fragment in 100 μl 0.1 M pyridine-acetate-collidine buffer, pH 8.3, was digested by carboxypeptidase A (type I-DFP; Sigma Chemical Co., St. Louis, MO) for 20 h at 37°C at a 5:1 molar ratio. The reaction was terminated with 50 μl acetic acid, and the solution was dried by SpeedVac and resolubilized in 100 μl 0.2 M citric acid (pH 2.2). Liberated amino acids were analyzed by HPLC using an AA-Pak column (Japan Spectroscopic Co., Ltd., Tokyo) with post-column o-phthalaldehyde derivatization (with the help of Dr. Masafumi Kamada, Department of Biochemistry, Science University of Tokyo), and quantitated using external amino acid standards. Controls were carboxypeptidase incubation without sample, and substitution of met-enkephalin (Tyr-Gly-Gly-Phe-Met) as a positive control.

Biological Assays

Cell spreading assays were performed in 96-well microtiter plates using fibroblastic BHK cells as described previously (54). Substrates were prepared either by coating tissue culture plates (Costar Laboratories) with solutions of fibronectin or fragments as described (54) or by covalently coupling fibronectin or its fragments to CovaLink plates (Nunc, Naperville, IL). To prepare covalently coupled substrates, triplicate CovaLink wells were treated with 100 μl of 1 mg/ml bis(sulfo-succinimidyl) suberate cross-linking reagent (BS3;[1] Pierce Chemical Co., Rockford, IL) in PBS+ for 30 min at 4°C. After washing, the wells were incubated with 100 μl of various concentrations of fibronectin or fragments for 1 h at room temperature. Background spreading was minimized by first incubating the wells with 0.15 M glycine for 30 min, followed by a 30-min incubation with 1% heat-denatured BSA, prepared as described (54). The plates were extensively washed with PBS+ before use. One well of each triplicate set was used to assay cell spreading activity. The remaining two wells of each set were used to quantitate amounts of each protein covalently coupled in the wells by ELISA using 5 μg/ml mAb 333 as the first antibody in PBS+ supplemented with 0.15 M glycine and 0.1% BSA.

1. *Abbreviation used in this paper*: BS3, bis(sulfosuccinimidyl) suberate.

Cell migration assays were performed using the procedure described previously (3,50). Fibronectin matrix assembly assays using WI-38 human embryonic lung fibroblasts were carried out as described (3). Fibronectin matrices stained with FITC-labeled antihuman fibronectin antibodies were photographed using identical exposure times for all treatment conditions with Kodak Tri-X film in a Zeiss Photomicroscope III using a 63×, 1.4 NA objective. Matrix assembly was quantitated by counting the numbers of fibrils observed to be crossing a straight line of arbitrary fixed length (100 μm on each field) drawn across randomly selected microscope fields.

ELISA

The ELISAs were carried out by incubating protein coated wells of either Immunolon-1, Costar, or CovaLink microtiter plates with 100 μl of either hybridoma-conditioned medium or purified antifibronectin mAbs in 0.5% Tween-20 in PBS (incubation buffer) for 2 h at room temperature followed by washing with incubation buffer. In experiments where Immulon-1 or Costar plates were used, HRP-conjugated, affinity purified anti-rat IgG (ICN Immunobiologicals, Costa Mesa, CA) at a 1:200 dilution in incubation buffer was used as the secondary antibody. After washing, peroxidase substrate in the form of 2 mM 2,2′-azino-bis(3-ethylbenzthiazoline-6-sulfonic acid) (ABTS), 2.5 mM H_2O_2 in 0.1 M sodium acetate, 0.05 M NaH_2PO_4, 0.01% thimerosal was added and reaction product was quantitated at 405 nm. When CovaLink plates were used, the secondary antibody was biotin-labeled anti-rat IgG (ICN Immunobiologicals) diluted 1/300 in incubation buffer. The wells were washed again with incubation buffer and 100 μl of a 1/200 dilution of HRP-conjugated avidin (ICN Immunobiologicals) was added for 1 h, followed by further washing and addition of peroxidase substrate.

Production and Characterization of mAbs against the 37-kD Fragment

Hybridomas secreting anti-37-kD fragment mAbs were produced by the fusion of Y3 rat myeloma cells with spleen cells from a Sprague-Dawley rat as described (15). The rat had been previously immunized with highly purified 37-kD fragment by intraperitoneal injection with complete Freund's adjuvant and boosted with the 37-kD fragment in incomplete Freund's adjuvant. Positive clones were identified by ELISA using 100 μl hybridoma conditioned medium as the first antibody. ELISA substrates were prepared by incubating 5 μg/ml 37-kD fragment with 96-well Costar tissue culture clusters and then blocking with 0.1% crystalline BSA. The positive hybridomas were subcloned twice by limiting dilution and isotyped using a Rat MonoAb-ID/SP kit (Zymed Laboratories, Inc., San Francisco, CA). For the large-scale production of antibodies, the hybridomas were cultured in serum-free medium supplemented with BSA and ITS Premix (Collaborative Research, Bedford, MA) as described (2). mAbs were purified from hybridoma-conditioned serum-free medium by protein G affinity chromatography (Pierce Chemical Co.). All hybridomas selected for further experimentation were subcloned at least twice by limiting dilution.

Epitope mapping of mAbs was carried out by ELISA using fusion proteins expressed by the λgt11 system in *E. coli* based on recombinant DNA mutagenesis of fibronectin (38; footnote 2). After affinity purification using mAb 333-Sepharose columns (38), the fusion proteins or fibronectin fragments were coated onto Immulon-1 plates (Dynatech Laboratories, Inc., Chantilly, VA) at 5–10 μg/ml in PBS+ for 1 h at room temperature, then subjected to ELISA usually using purified IgG at 50 μg/ml or, in some cases, hybridoma-conditioned medium containing 40 to 50 μg/ml IgG.

mAb binding competition assays were carried out as described above for the standard ELISAs using fibronectin-coated Costar 96-well plates. The wells were preincubated with one of each of the unlabeled mAbs for 1 h. Then mAbs that had been directly labeled with HRP were added for 1 h. After extensive washing, binding of labeled mAb was quantitated as described for the standard ELISA. Purified mAbs were labeled directly with HRP using preactivated peroxidase in the form of ActiZyme-HRP (Zymed Laboratories, Inc.) according to the manufacturer's instructions. Affinity constants of mAb binding to fibronectin were determined by radioimmunoassay using the procedure of Frankel and Gerhard (14).

Other Methods

Protein concentrations were determined by the BCA protein assay (Pierce Chemical Co.) using BSA as a standard. SDS-PAGE was performed as described (29), using a 4% stacking gel and 10% resolving gel. Proteins were transferred to nitrocellulose membrane (Schleicher & Schuell, Keene NH) as described (7). Protein bands were localized either by staining with 2% Amido Black 10B or with mAb 333. Blots used for mAb detection of fibronectin fragments were blocked for 30 min with 5% nonfat dry milk solids in PBS+, and immunostaining was carried out using mAb 333 and HRP-conjugated, affinity-purified rabbit anti-rat IgG (ICN Immunobiologicals) as first and second antibodies, respectively. HRP activity was localized using 5 mg/ml 3,3′-diaminobenzidine, 0.01% H_2O_2 in 0.1 M Tris-HCl, pH 7.4.

Results

Purification and Characterization of a 37-kD Cell-binding Fragment

Previous reports have described proteolytic cell-binding fragments derived from the central portion of fibronectin and containing the Arg-Gly-Asp cell recognition site ranging in size from 11.5 up to 120 kD (2, 19, 41, 17a, 46, 47, 57). Whereas the larger fragments bind to cells with similar affinities as the intact molecule, the small 11.5-kD fragment has been found to bind to cells with a markedly lower affinity (2). We have used a partial chymotrypsin digestion followed by chromatographic methods to generate a fibronectin cell-binding fragment that would be of an intermediate size between those of the fully active 75-kD fragment and the low affinity 11.5-kD fragment. As shown in Fig. 1 (lane *2*), a homogenous fragment with an estimated size of 37 kD was obtained after purification. This fragment was recognized by mAb 333, which binds to the previously described 11.5-kD cell-binding fragment and inhibits cell attachment to the Arg-Gly-Asp site (2,21).

The sequence of the first 20 amino acids of the 37-kD fragment was found to be Thr-Val-Lys-Asp-Asp-Lys-Glu-Ser-Val-Pro-Ile-Ser-Asp-Thr-Ile-Ile-Pro-Ala-Val-Pro (TVKDDKESVPISDTIIPAVP), in complete agreement with the known human fibronectin sequence as deduced from cDNA analysis starting at residue 1218 and lacking the ED-B (EDb or EIIIb) sequence (28,36). Analysis of the first few amino acid residues was entirely unambiguous, suggesting that the 37-kD fragment had been purified to homogeneity as indicated by the electrophoretic analysis in Fig. 1. The amino-terminal

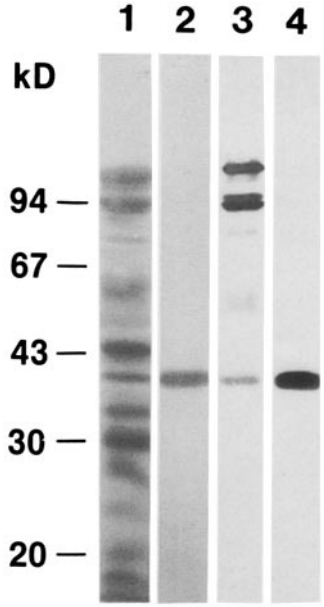

Figure 1. Western blot analysis of chymotryptic digest of fibronectin and purified 37-kD cell-binding fragment. Fragments generated by treating human plasma fibronectin with chymotrypsin (lanes *1* and *3*) or purified 37-kD fragment (lanes *2* and *4*) were resolved by electrophoresis on a 10% polyacrylamide gel under nonreducing conditions followed by electroblotting to nitrocellulose. Fragments were stained with either amido black (lanes *1* and *2*) or mAb 333 (which binds close to the RGD site of fibronectin) and HRP-labeled anti-rat IgG serum (lanes *3* and *4*). The relative positions of molecular weight standards are indicated on the left.

sequence of this 37-kD fragment exactly matched that of a 34-kD fragment from bovine fibronectin isolated by Skorstengaard et al. (47) after extensive digestion with chymotrypsin. Analysis of carboxy-terminal amino acids by carboxypeptidase A treatment and amino acid analysis yielded 214 pmol Met and 174 pmol Gln from an initial 300 pmol of 37-kD fragment, indicating that the 37-kD human fragment has the same carboxy-terminal Gln-Met sequence as the bovine fragment (47). This fragment therefore starts at residue 1218 (Thr_{1218}), lacks the ED-B domain, and terminates at the methionine at residue 1517 (using the published nomenclature omitting the ED-B sequence: refs. 28 and 47)[2].

Biological Activity of the 37-kD Fragment

The ability of solubilized 37-kD fragment to inhibit BHK fibroblastic cell spreading on fibronectin substrates was compared to that of the 11.5-kD fragment and synthetic GRGDS peptide. As shown in Fig. 2, the 37-kD fragment, the 11.5-kD fragment, and GRGDS peptide could all inhibit cell spreading on fibronectin with half-maximal inhibition occurring at concentrations of 47 μg/ml (1.2×10^{-6} M), 850 μg/ml (74×10^{-6} M) and 190 μg/ml (390×10^{-6} M), respectively. Thus, on a molar basis, the 37-kD fragment was 325-fold more active than the GRGDS peptide and 60-fold more active than the 11.5-kD fragment in this assay. These results indicate that information present in the 37-kD fragment, but lacking from the 11.5-kD fragment and synthetic peptide, is important for biological activity.

To compare directly the relative cell spreading activities of fibronectin and fragments, substrates were prepared by covalently coupling either intact fibronectin, the 37-kD fragment, or the 11.5-kD fragment to CovaLink activated polystyrene 96-well assay plates, and the relative amounts of each protein were measured by ELISA using duplicate parallel wells as described in Materials and Methods. The data, shown in Fig. 3, were plotted as the percentage of spread cells as a function of the relative amount of moles of fibronectin or fragment actually present on the substrate. This experiment showed that the 37-kD fragment had essentially the same cell spreading activity as fibronectin itself on a molar basis. The activity of the 11.5-kD fragment was very low, suggesting that the 11.5-kD fragment lacks information contained in the 37-kD fragment required for complete interaction with fibroblastic cells.

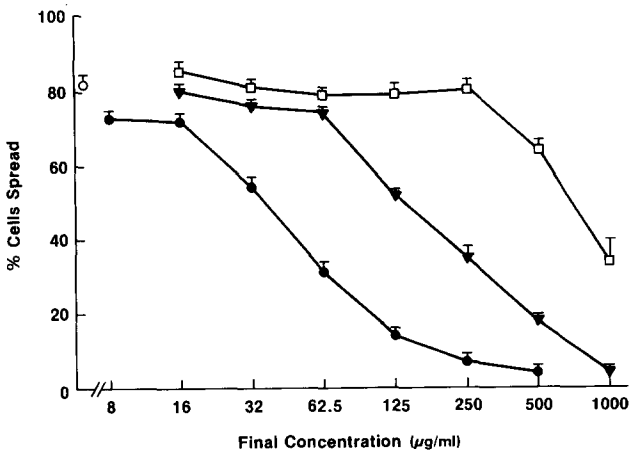

Figure 2. Comparison of the relative inhibitory activities of the 37- and 11.5kD cell-binding fragments and GRGDS synthetic peptide on spreading of BHK fibroblasts. BHK cells were incubated in 96-well tissue culture clusters coated with 2 μg/ml fibronectin in the presence of the indicated concentrations of 37-kD fibronectin cell-binding fragment (●), 11.5-kD fibronectin cell-binding fragment (□), or GRGDS peptide (▼). The open circle indicates the percent cells spread in control wells containing no inhibitor. Each point indicates the average percentage of cells spread from 10 random fields (100 cells counted/field) ± SEM.

Characterization of mAbs Raised Against the 37-kD Fragment

Five hybridoma clones designated 11E5, 3B8, 13G12, 12B4, and 16G3 were selected for use in this study. All of these hybridoma clones secreted antibodies of the IgG_1 subclass. The epitope of each mAb was analyzed by ELISA using a

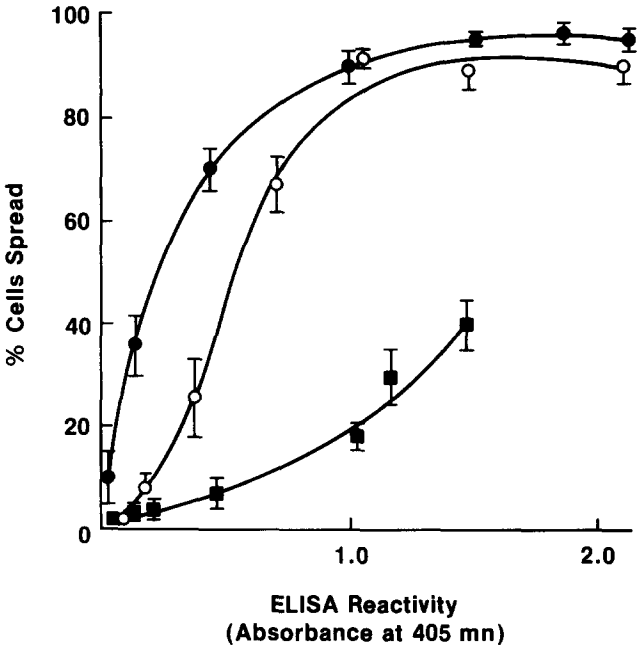

Figure 3. Spreading of BHK cells on substrates prepared by covalently cross-linking fibronectin or cell-binding fragments to plastic. Fibronectin (○), 37-kD (●), or 11.5-kD (■) cell-binding fragments at various concentrations ranging from 0.03 to 4.0 μg/ml were coupled to Nunc Covalink wells using BS3 homobifunctional cross-linking reagent and were assayed for BHK cell-spreading activity. Each point indicates the average percentage of cells spread from 10 random fields (100 cells counted/field) ± SEM. The relative amount of each protein present in the wells as measured by the ELISA method on parallel duplicate wells is indicated on the abscissa in units of absorbance at 405 nm.

2. Using terminology based on the presently known full sequence (22, 36), the carboxy-terminal residue of the 37-kD fragment is Met_{1608}. This fragment contains the terminal 17 amino acids of the fibronectin repeating unit III-7, the entirety of III-9, III-10, and III-11, and eight amino acids of III-12. Its theoretical molecular size from the sequence of human plasma fibronectin in the absence of posttranslational modification would be 33 kD (28). For comparison, the 11.5-kD fragment extends from Ile_{1501} to the same Met_{1608} in the currrent full sequence nomenclature (36, 39, 41), and it consists primarily of unit III-11 (with the carboxy-terminal end of III-10 and the amino-terminal end of III-12).

Table I. Epitope Mapping by ELISA

mAb	Residue number	
	Positive	Negative
11E5	1217	1260
3B8	1355	1359
13G12	1359	1363
12B4	1363	1368
333	1384	1429
16G3	1429	–

The epitopes for each of the mAbs generated in this study and for the previously described mAb 333 were mapped on the 37-kD fibronectin cell-binding fragment by ELISA using a variety of deletion mutants in the form of β-galactosidase fusion proteins expressed in the λgt11 bacterial expression system (38; footnote 2). The values in the table indicate the last amino acid residue present at the boundaries of the fibronectin sequence deletions from the amino terminus. For example, mAb 11E5 showed positive ELISAs for deletions extending up to (but not ncluding) residue 1234, but this mAb was negative for binding to adjacent deletion mutants, the closest of which retained residue 1260. The binding site for mAb 16G3 was the most carboxyl terminal. The epitope for mAb 11E5 was also mapped for its carboxyl-terminal boundary, which was residue 1329. All residue numbers are based on the numbering system for fibronectin of entry FNHU, accession number A03213, in the NBRF PIR (Protein Identification Resource) databank, which omits the ED-B (EIIIB) alternatively spliced domain and matches the notation of previous mutants (38). Another method of mapping is based on numbering the 17 known type III repeats of fibronectin consecutively (ED-B would be numbered III-8 according to the nomenclature of ref. 36, p. 4). Although further mapping is needed to determine exact epitope boundaries, mAb 11E5 appears to bind to III-9; 3B8, 3G12, and 12B4 bind to portions of III-10 and possibly III-11; 16G3 recognizes III-11; and 333 binds III-10 and/or III-11.

series of fibronectin fragments and bacterially expressed fibronectin fusion proteins. All mAbs bound to intact fibronectin, the 37-kD fragment, and the clone 6 fusion protein which overlaps the entire sequence of 37-kD fragment (38). Only mAb 16G3 and the control mAb 333 bound to the 11.5-kD fragment, indicating that the epitopes of mAb 333 and mAb 16G3 are both located near the carboxy-terminal region of the 37-kD sequence, close to the RGD site. mAb 11E5 did not bind to clone 18 which overlaps all of the 37-kD fragment except the amino-terminal region (38), indicating that the epitope of this mAb was located in the most amino-terminal region. Further analyses were carried out using a series of fibronectin fusion proteins with known deletions. Thus, the epitope of mAb 11E5 was mapped ~11 kD from the amino terminus of the 37-kD fragment, those for mAbs 3B8, 13G12, and 12B4 are in sequence from the amino to the carboxy terminus, and the epitope for mAb 16G3 is closer to the Arg-Gly-Asp site than mAb 333 (Table I).

All of the mAbs were further tested by ELISA for competitive inhibition of binding to fibronectin between HRP labeled coupled mAbs and nonlabeled mAbs (Table II). Each unlabeled mAb completely inhibited binding of its HRP-labeled counterpart. mAbs 13B12 and 12B4 were found to compete for similar binding sites. No other pair of mAbs was found to compete for binding. These results indicate that the five mAbs recognize four distinct epitopes. The results of the epitope mapping experiments are summarized in Fig. 4 (*top*).

Immunological Mapping of Two Separate Regions Required for Cell Adhesion

The biological activities of each mAb were examined in three different assays to evaluate fibronectin functions in cell spreading, cell migration, and matrix assembly. As shown in Fig. 4 (*bottom*), mAbs 3B8 and 16G3 were both found to inhibit BHK cell spreading, requiring only ~10 μg/ml for half-maximal inhibition. Similarly, half-maximal inhibition of HT-1080 fibrosarcoma cell spreading was also obtained with mAbs 3B8 and 16G3 at ~10 μg/ml. These two mAbs also inhibited BHK cell spreading on the 37-kD fragment itself, whereas even 100 μg/ml of each did not affect spreading on 5 μg/ml vitronectin (data not shown). In contrast to the inhibitory activity of mAbs 3B8 and 16G3 on fibronectin, mAbs 11E5, 13G12, and 12B4 had minimal inhibitory activity in this assay, even at concentrations of 100 μg/ml (Fig. 4). The inhibitory activity of mAb 16G3 can be explained by the proximity of its epitope to the Arg-Gly-Asp site. However, the inhibition by the mAb 3B8 can only be easily explained by its blocking of a second cell adhesion site within the 37-kD fragment. It is important to note that in this experiment, mAb 13G12 (and to a lesser extent 12B4), which bound to sites on the 37-kD fragment between those for the two inhibitory mAbs, can be considered negative controls that rule out possible steric effects of the inhibitory antibodies and that demonstrate separability of the two sites.

One possible trivial explanation of the cell spreading data is that the inhibitory mAbs bound to fibronectin with high affinity and the noninhibitory mAbs bound with low affinity. To rule out this possibility, the binding constant of each mAb for fibronectin was determined by radioimmunoassay. The inhibitory mAbs 3B8 and 16G3 were found to have estimated K_d values for fibronectin coated onto the plastic substrate of 1.3×10^{-9} and 1.0×10^{-9} M, respectively. The noninhibitory antibodies 11E5, 13G12, and 12B4 were found

Table II. Mutual Competition Binding Profiles of Anti-37-kD mAbs by ELISA

Nonlabeled mAbs	Labeled mAbs				
	11E5	3B8	13G12	12B4	16G3
11E5	2 ± 1	83 ± 7	101 ± 2	98 ± 2	105 ± 7
3B8	110 ± 6	1 ± 0	107 ± 1	113 ± 4	91 ± 1
13G12	88 ± 7	103 ± 5	1 ± 1	1 ± 0	115 ± 12
12B4	91 ± 7	97 ± 6	2 ± 0	1 ± 1	103 ± 8
16G3	116 ± 5	105 ± 9	108 ± 2	120 ± 5	1 ± 1

Competitive inhibition of binding between HRP-labeled mAbs and nonlabeled mAbs in all combinations was tested by ELISA. Aliquots of fibronectin coated onto Costar plates at a concentration of 5 μg/ml solution were preincubated with each of the nonlabeled mAbs (100 μl at 50 μg/ml) for 3 h at room temperature. Subsequently, 10 μl of HRP-labeled mAb (50 μg/ml) was added to each well and the antibodies were coincubated for 1 h at room temperature (nonlabeled mAb/labeled mAb = 10:1). After washing, the activity of the HRP on the labeled mAbs bound to fibronectin was measured. Data were expressed as percentage of total absorbance observed without nonlabeled mAb (noncompeted control) for each mAb, which were as follows: 11E5, 1.86 ± 0.05 absorbance units; 3B8, 2.22 ± 0.12; 13G12, 1.99 ± 0.03; 12B4, 1.62 ± 0.01; and 16G3, 1.98 ± 0.06. All values represent the mean ± SEM of four assays.

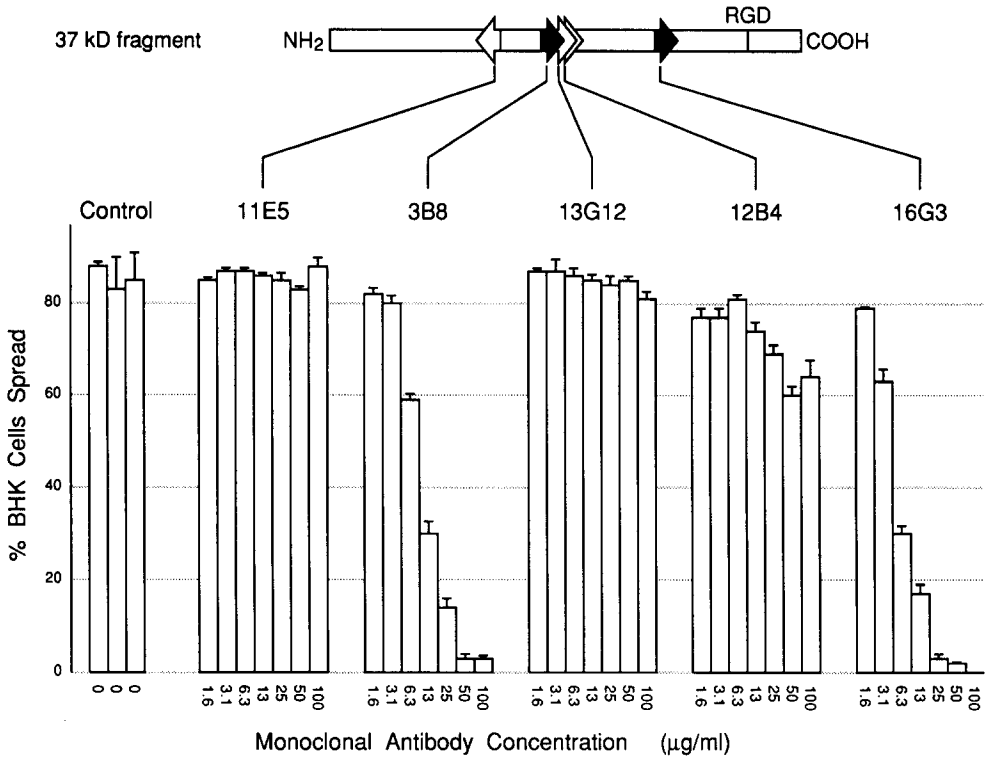

Figure 4. Biological activities and map of the epitopes of the anti-37-kD mAbs. (*top*) The estimated epitope recognition site of each mAb as mapped by ELISA analysis of fusion proteins and fragments is indicated along the 37-kD sequence; see Table I for numerical mapping data. The solid arrows indicate the active mAbs and the open arrows indicate the inactive mAbs as determined by cell spreading assays. (*Bottom*) Inhibition of BHK cell spreading by each of the anti-37-kD fragment mAbs on fibronectin substrates. Tissue culture clusters coated with 2 μg/ml fibronectin were pretreated for 60 min with 50 μl of the various mAbs. Then 25 μl of BHK cell suspension containing 1×10^4 cells were added to the wells to yield the indicated final concentrations of mAbs. Each bar represents the average of ten determinations from random fields (100 cells/field) of duplicate wells ± SEM.

to have estimated K_d values of 1.2×10^{-9}, 1.2×10^{-10}, and 1.6×10^{-10} M, respectively. Thus, differences in the apparent affinity of the mAbs cannot account for the observed differences in biological activity, and the simplest interpretation of the data is that mAb 3B8 inhibits cell spreading by binding to a second, crucial cell-binding site ~15 kD distant from the RGD site in the NH_2-terminal direction on fibronectin.

Immunological Mapping of Sites Required for Cell Migration

Besides mediating adhesion, fibronectin can also promote migration by a variety of cell types. Fig. 5 shows that mAbs 3B8 and 16G3 at 200 μg/ml strongly inhibited cell migration by HT-1080 cells on fibronectin (72 and 84% inhibition, respectively; both values were statistically significant at the $p < 0.001$ level); half-maximal inhibition was observed at ~2 μg/ml of each of these two antibodies (data not shown). The inhibition of migration in this outgrowth assay was confirmed by time-lapse video microscopy: both mAb 3B8 and mAb 16G3 strongly inhibited the migration of HT-1080 cells as determined by following the paths of individual cells, whether they existed as single cells or as aggregates of cells in contact; although cells treated with these two mAbs remained attached to the fibronectin substrate, they moved back-and-forth randomly in place rather than undergoing directed translocation (data not shown). In outgrowth assays conducted in parallel to these anti-37-kD experiments, similarly high levels of inhibition of migration (75–100%) were obtained with mAb 16, a mAb that specifically inhibits function of the $\alpha_5\beta_1$ fibronectin receptor in cell migration by this particular cell on fibronectin (data not shown; see also refs. 3 and 55).

In contrast, mAb 13G12 did not significantly inhibit migration (Fig. 5), even though the epitope for this mAb lies between those of the two highly active mAbs. mAb 12B4 reproducibly showed substantial but not complete inhibitory activity in these cell migration assays (60% inhibition, significant at the $p < 0.001$ level). Although minimal inhibitory activity was observed for this particular mAb in the BHK cell spreading assay for cell adhesion (see Fig. 4), significant activity was also found in parallel spreading assay conducted with the HT-1080 cells used for the cell migration assays (50% inhibition; Fig. 6).

Immunological Mapping of Sites Required for Fibronectin Matrix Assembly

Regions of the central cell-binding domain of fibronectin molecule required for its assembly into a fibrillar matrix were mapped by incubating human WI-38 fibroblasts with each mAb during the process of matrix assembly over a period of 24 h. As shown in Fig. 7, mAb 3B8 that binds to the putative synergy region inhibited strongly, and mAb 16G3 that binds close to the RGD site was also inhibitory, whereas the three other mAbs had little or no effect on this process. Direct quantitation of fibrillogenesis as shown in Fig. 8 showed that mAb 3B8 inhibited fibril formation by 75%, while mAb 16G3 inhibited by 63% at 200 μg/ml ($p < 0.001$ for both antibodies). Half-maximal inhibition of fibrillogenesis occurred at ~20 μg/ml for mAb 3B8 and at

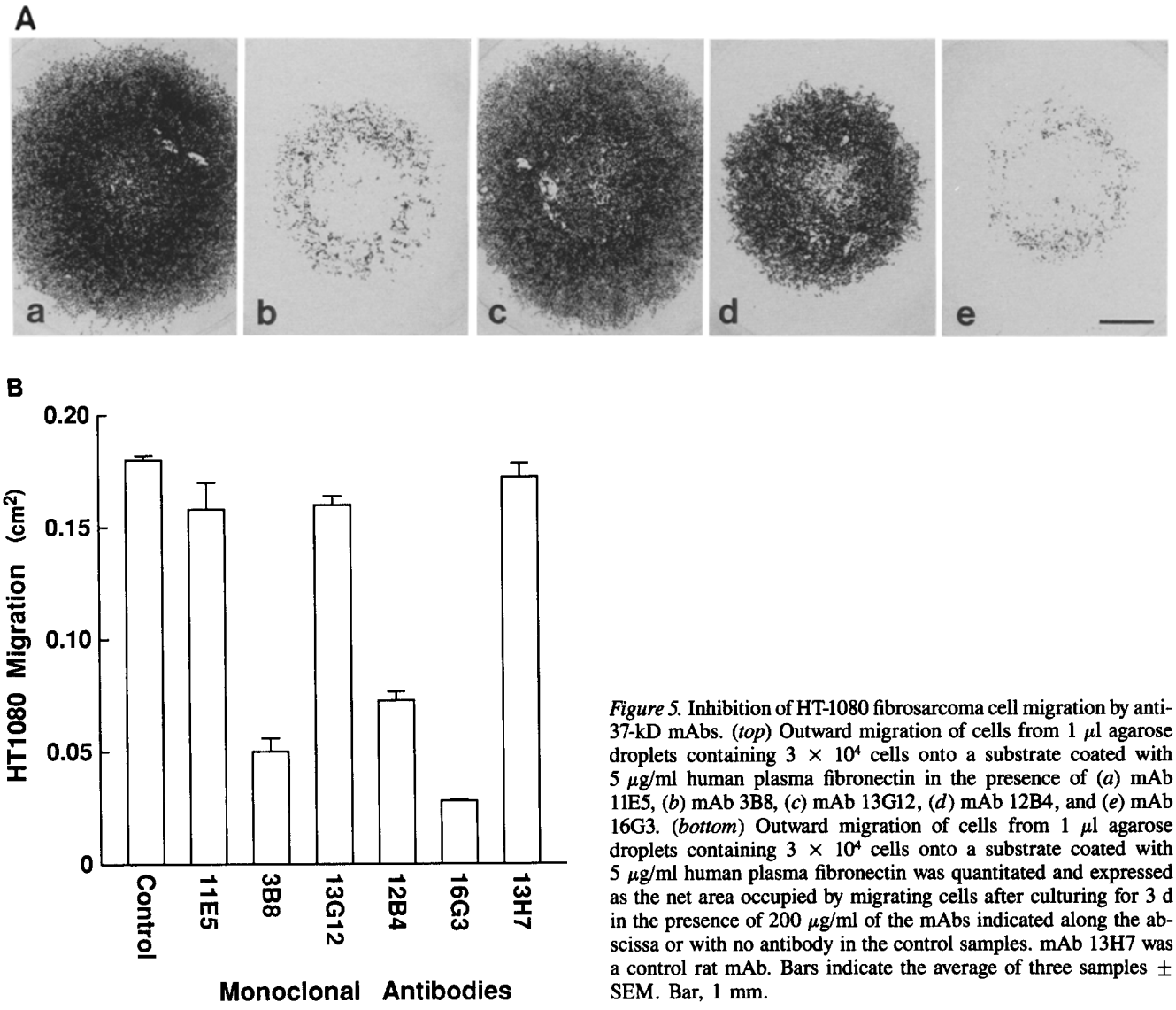

Figure 5. Inhibition of HT-1080 fibrosarcoma cell migration by anti-37-kD mAbs. (*top*) Outward migration of cells from 1 μl agarose droplets containing 3 × 10^4 cells onto a substrate coated with 5 μg/ml human plasma fibronectin in the presence of (*a*) mAb 11E5, (*b*) mAb 3B8, (*c*) mAb 13G12, (*d*) mAb 12B4, and (*e*) mAb 16G3. (*bottom*) Outward migration of cells from 1 μl agarose droplets containing 3 × 10^4 cells onto a substrate coated with 5 μg/ml human plasma fibronectin was quantitated and expressed as the net area occupied by migrating cells after culturing for 3 d in the presence of 200 μg/ml of the mAbs indicated along the abscissa or with no antibody in the control samples. mAb 13H7 was a control rat mAb. Bars indicate the average of three samples ± SEM. Bar, 1 mm.

40 μg/ml for mAb 16G3; similar patterns of inhibition were observed using a previously described immunoblotting protocol (3; data not shown). mAb 333, which also binds close to the RGD site (though not as closely as mAb 16G3), also inhibited matrix assembly by 73% (Fig. 8). There were only minimal amounts of inhibition by control mAbs that did not reach statistically significant levels, including by the mAbs located between the two active sites: mAb 13G12 showed 8% inhibition ($p = 0.5$), and mAb 12B4 showed only 15% inhibition ($p = 0.3$) in comparison with the untreated control (Fig. 8). As reported previously (3), mAb 16 and mAb 13 against the α and β subunits of the $\alpha_5\beta_1$ fibronectin receptor also inhibited fibrillogenesis in this newer assay (Fig. 8; 75% inhibition). mAb 13 was the most effective of all mAb inhibitors in this assay, inhibiting fibril formation by 86% (Fig. 8). These levels of inhibition can be compared with the 75% inhibition by 3B8. Interestingly, the maximal concentrations of the anti-$\alpha_5\beta_1$ fibronectin receptor antibody and the antifibronectin synergy region antibody resulted in similar levels of inhibition (both inhibited 75 ± 5%), whereas the anti-β_1 antibody mAb 13 showed additional inhibition (86 ± 4%).

Discussion

We have purified and characterized a 37-kD fragment of fibronectin that was found to retain cell adhesive activity similar to that of intact fibronectin. This human fibronectin fragment corresponds in structure to a protease-resistant fragment of bovine fibronectin sequenced by Skorstengaard et al. (47) containing the 9th through 11th type III repeats of fibronectin. Its resistance to proteolysis suggests that it possesses considerable structure, rather than existing as a linear polypeptide. Using this fragment as an immunogen, we have generated a panel of mAbs that bind to four distinct epitopes found in the 37-kD fragment. Applying these antibodies as functional probes, we find that two distinct regions of the central cell-binding domain are important for fibronectin-mediated cell spreading and migration, and also for the assembly of extracellular fibronectin fibrils. One region appears to involve the Arg-Gly-Asp site. The second region maps a substantial distance away from the RGD site, to a location estimated to be ≤15 kD of polypeptide sequence toward the amino terminus. This site, which is inhibited by

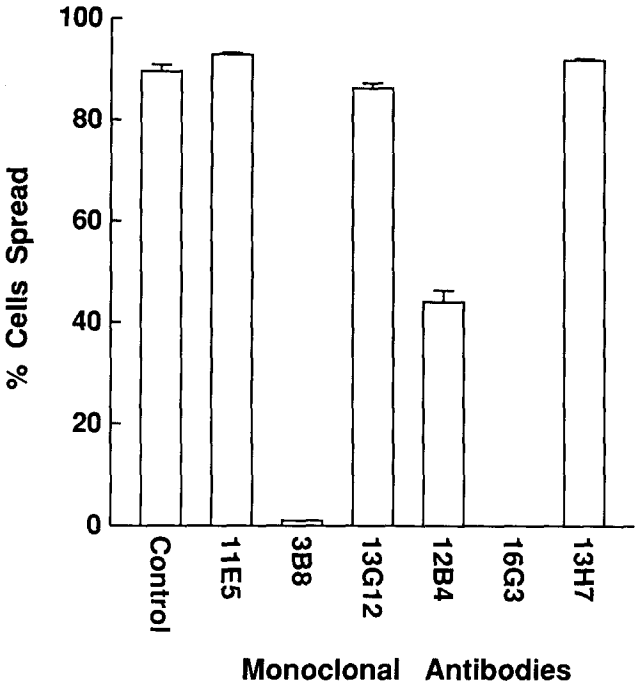

Figure 6. Inhibition of HT-1080 fibrosarcoma cell spreading by anti-37-kD mAbs. Tissue culture clusters (96-well) coated with 5 μg/ml fibronectin were pretreated for 60 min with 50 μl of the various mAbs. Then 25 μl of HT-1080 cell suspension containing 1×10^4 cells were added to the wells to yield a final concentration of 200 μg/ml of each mAb. mAb 13H7 was a control rat mAb. Each bar represents the average of ten determinations from random fields (100 cells/field) ± SEM.

mAb 3B8, is flanked by epitopes to which other mAbs bind with high affinity, yet binding to these flanking sites is not inhibitory. For example, mAb binding to an epitope estimated to be ≥25 kD of polypeptide sequence away from RGD is not inhibitory, and an epitope with a boundary ≥14 kD away from RGD is also not inhibitory in various biological assays.

These distances can be compared with rougher estimates from previous studies based on adhesive activity of several truncation mutants of fibronectin expressed in bacteria (38) or on partially inhibitory activities of mAbs (26). Our previous study showed a loss of activity after truncation of fibronectin sequences ≥20 kD away (38). The mAb study mapped a partially active site 153–229 amino acid residues (17–25 kD) upstream from the RGD site (26). The finer mapping possible in the present study suggests that a particularly important region is located ~14–15 kD away from the RGD site, rather than the original rough estimates a greater distance away. This new estimate is of interest in that it moves the mapped site of this postulated second, synergy region away from the location of the alternatively spliced ED-B (EIIIA) site, reducing the likelihood that alternative splicing could directly affect the biological function of this region. Recent fine-structure mapping of the putative synergistic region by site-directed mutagenesis has confirmed that a major functional subregion corresponds to the binding site of mAb 3B8 (4a). A second, quantitatively less important subregion was mapped further toward the amino terminus (4a), corresponding to the originally described site of loss of activity (38) and possibly to the binding site of the partially active mAb described by Katayama et al. (26).

The 37-kD proteolytic fragment we describe is half the size of the smallest fragment previously reported to retain full biological activity (19). As such, it directly confirms the prediction from mutagenesis studies that at least 52% of the amino-terminal sequence of fibronectin is not necessary for cell adhesion. The sequences in fibronectin required for cell migration require further characterization. The Arg-Gly-Asp sequence of fibronectin and other molecules is thought to be required for the migration of certain embryonic and adult cells based on competitive inhibition studies (6, 10, 30, 48). More extensive studies of neural crest derivatives reveal complex requirements for sites besides the RGD sequence; these cells might use the CS1 alternatively spliced sequence, the synergy region, and other sequences in fibronectin for migration or neurite extension (11, 21, 31, 37).

In this study, we examined cell migration in a system where the requirements for migration were simpler. HT-1080 cells were chosen because of their marked dependence on the $\alpha_5\beta_1$ fibronectin receptor for migration (55). Under our present assay conditions, an antibody against either the α_5 or β_1 subunits blocks migration. Conversely, antibodies against either subunit can substitute for the ligand and serve as substrates for migration (55). Using this cell line, we find by antifibronectin mAb analysis that both the synergy region and the RGD region are important for migration mediated by this particular receptor. A mAb that binds to fibronectin between these regions with high affinity (mAb 13G12) is not inhibitory. Consistent with the results, preliminary binding studies indicate that 3B8, the mAb that binds to the synergy region, inhibits the binding of $\alpha_5\beta_1$ to a fibronectin cell-binding domain affinity column.

Extracellular matrix assembly is a complex process thought to be dependent on integrin receptors and on both an amino-terminal 70-kD domain and the central cell-binding domain of fibronectin (34, 36). Antibodies against the α subunit of the classical fibronectin receptor $\alpha_5\beta_1$ partially inhibit fibronectin matrix assembly (3), and transfection of this receptor into CHO cells substantially promotes matrix assembly (16). Nevertheless, at least one other β_1 integrin appears to be involved in matrix assembly, since full inhibition is obtained only by blocking the functions of all β_1 integrins (13). Our present results indicate that important sites are located in both the RGD region and the synergy region of fibronectin. mAbs against either of these sites strongly inhibit fibronectin matrix assembly. Interestingly, none of the antifibronectin mAbs alone inhibited matrix assembly to the same degree as the antiintegrin β_1 mAb, consistent with earlier findings that interactions of fibronectin with multiple β_1 integrins are required for proper fibril formation (13, 42).

A number of integrin receptors have been reported to bind to fibronectin, including $\alpha_3\beta_1$, $\alpha_5\beta_1$, $\alpha_v\beta_3$, and $\alpha_v\beta_1$. Direct binding to the RGD motif is thought to explain the function of many of these fibronectin receptors (4, 5, 8, 12, 17, 20, 22, 23, 25, 36). It is interesting to compare the requirements for different receptors for differing cellular functions involving fibronectin; initial cell attachment to fibronectin often involves the classical $\alpha_5\beta_1$ receptor. Cell spreading on fibronectin can require this receptor (55) or proceed quite well

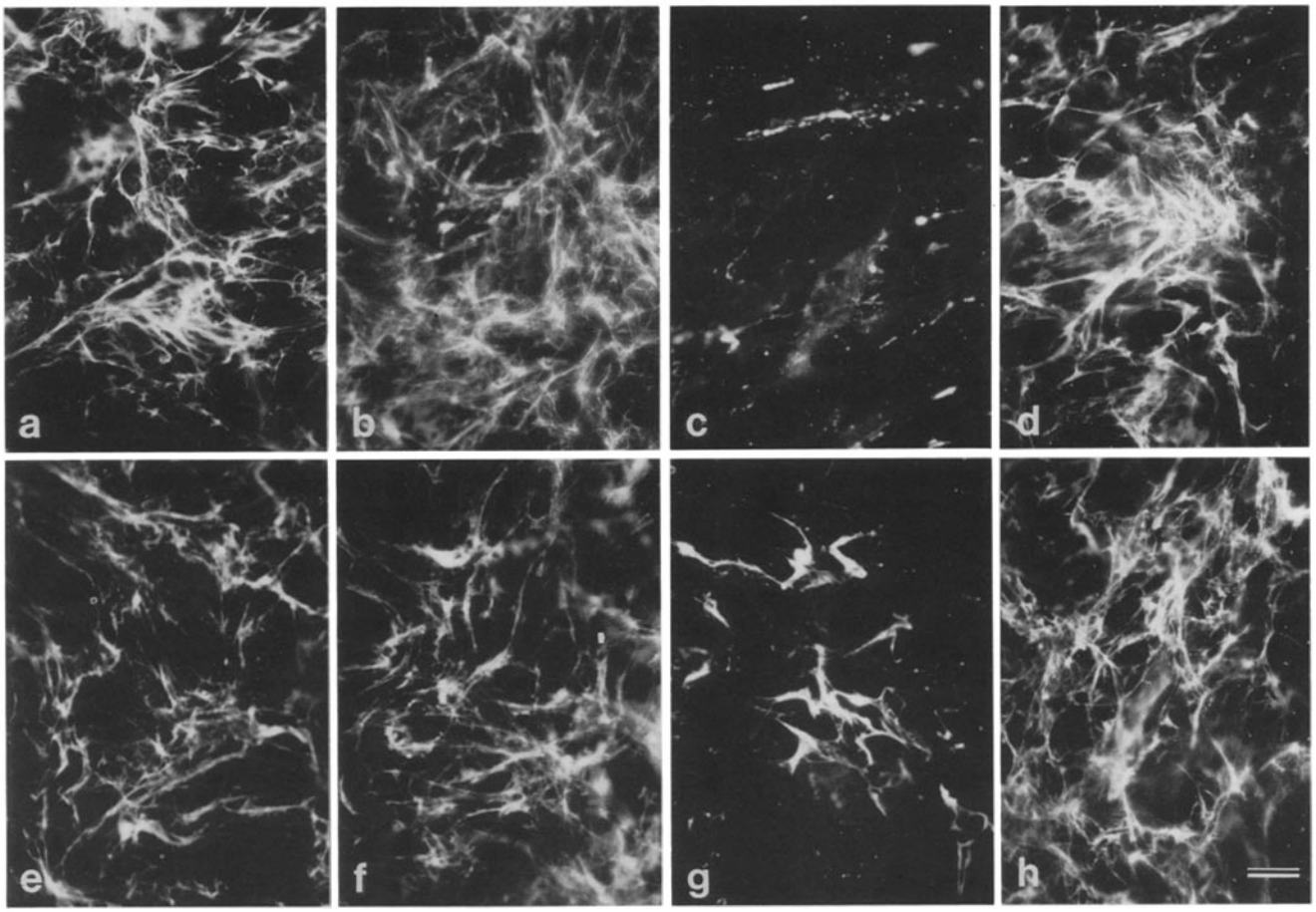

Figure 7. Inhibition of fibronectin extracellular matrix assembly by anti-37-kD mAbs. WI-38 human lung fibroblasts were cultured for 24 h with or without the indicated mAbs at 200 μg/ml, then fixed, permeabilized, and stained with FITC-labeled rabbit antihuman fibronectin antibody as described previously (3). These immunofluorescence micrographs were taken and printed using identical exposure times to permit direct comparisons. (*a*) Untreated control; (*b*) mAb 11E5; (*c*) mAb 3B8; (*d*) untreated control; (*e*) mAb 13G12; (*f*) mAb 12B4; (*g*) mAb 16G3; (*h*) control rat mAb 13H7. Bar, 20 μm.

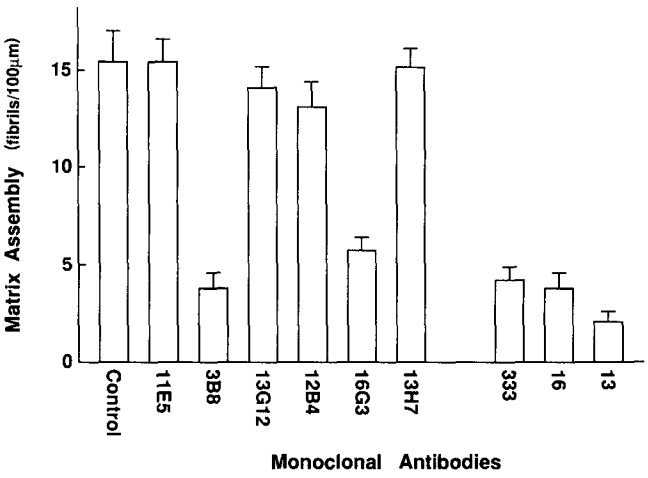

Figure 8. Quantitation of the inhibition of fibronectin matrix assembly by mAbs. WI-38 fibroblasts were cultured for 24 h in the presence of 200 μg/ml of the indicated mAbs, and then stained with FITC-labeled antifibronectin antibody. Fibrils observed to cross a line of fixed length in random microscopic fields were counted for each experimental condition. Bars indicate the average of data from 10 random fields for each condition showing numbers of fibrils per 100 μm ± SEM.

in other cells such as WI-38 fibroblasts even if it is inhibited (4). Migration on fibronectin can be inhibited by antibodies to this receptor in HT-1080 cells and others, yet WI-38 fibroblasts show no inhibition or even an augmentation of migration rates. Fibronectin matrix assembly is partially dependent on $\alpha_5\beta_1$, yet may also require other β_1 integrins (4, 13, 16, 42).

This complex picture is further complicated by the question of whether more than the RGD site is needed for various functions. Mutagenesis studies have implicated a second, synergistic site in cell adhesion to fibronectin by BHK cells (27, 38). Such studies are undermined by concerns about the effects of mutations on polypeptide conformation, which may help to explain the discrepancies between these investigations (compare refs. 27, 38, and footnote 2). This study provides independent, immunological evidence for the role of a second region in the central cell-binding domain of fibronectin that is involved not only in cell adhesion, but in at least two other major functions of the protein. The fact that this epitope located distant from the RGD site, but not one or two intervening epitopes, is implicated in three different processes involving cell interactions with fibronectin indicates that this region is a functional site that either binds directly to one or more key receptors, or must be in close

proximity. In contrast, one or two intervening fibronectin sequences are apparently not close in the folded protein. The slightly different profile of inhibition for cell migration as opposed to matrix assembly involving increased relative sensitivity of migration to 12B4 (Fig. 5) suggests the possibility of slightly different types of receptor interaction with this synergistic region of fibronectin.

An attractive but unproven hypothesis that could explain all of our immunological and mutagenesis results, is that the $\alpha_5\beta_1$ fibronectin receptor binds directly to both the RGD site and the synergistic region. Approaches to evaluate this hypothesis would include determination of the three-dimensional molecular structure of the entire fibronectin cell-binding domain by x-ray crystallography or nuclear magnetic resonance spectroscopy, as well as chemical crosslinking experiments. It is of interest that an x-ray inactivation study attempting to determine the minimal functional size of the cell-binding site of the fibronectin molecule estimated a polypeptide target size of 32 kD, rather than only the RGD tripeptide sequence (56). This target size of 32 kD is quite close to that of the 34–37-kD protease-resistant domain described by Skorstengaard et al. (47) and characterized biologically and immunologically in the present paper.

Our characterization of the mAb 3B8 site does not exclude the possibility that other cell-binding sites in the fibronectin molecule can be important for cell adhesion. The cell-binding site located in the IIICS region (21) is important for the adhesion of melanoma cells and other cells derived from the neural crest. The adhesion-promoting sites in the heparin-binding domain can also be important for certain cell types, especially for the formation of focal contacts and microfilament bundles (24, 32, 51). Although none of these other sites have been shown to interact with the high affinity $\alpha_5\beta_1$ integrin fibronectin receptor as do the sites contained in the 37-kD fragment, it will be important to extend studies on fibronectin-mediated cell adhesion to determine if any or all of these various cell interaction sites on fibronectin can interact in an independent, cooperative, or synergistic fashion.

We thank Dorothy W. Kennedy and Masae Nagai for their valuable technical assistance and Dorothea Dudek for her assistance in the preparation of this manuscript.

This work was supported in part by National Institutes of Health grants CA-14718 and CA-45290, American Cancer Society Grant CD-452C, and a Faculty Research Support Grant awarded to K. Olden, and National Institutes of Health grant CA-45515 and a Faculty Research Support Grant awarded to S. K. Akiyama.

Received for publication 8 February 1991 and in revised form 24 May 1991.

References

1. Akiyama, S. K., and K. M. Yamada. 1987. Fibronectin. *Adv. Enzymol.* 57:1–57.
2. Akiyama, S. K., E. Hasegawa, T. Hasegawa, and K. M. Yamada. 1985. The interaction of fibronectin fragments with fibroblastic cells. *J. Biol. Chem.* 260:13256–13260.
3. Akiyama, S. K., S. S. Yamada, W. -T. Chen, and K. M. Yamada. 1989. Analysis of fibronectin receptor function with monoclonal antibodies: role in cell adhesion, migration, matrix assembly, and cytoskeletal organization. *J. Cell Biol.* 109:863–975.
4. Akiyama, S. K., K. Nagata, and K. M. Yamada. 1990. Cell surface receptors for extracellular matrix components. *Biochim. Biophys. Acta.* 1031:91–109.

4a. Aota, S., T. Nagai, and K. M. Yamada. 1991. Characterization of regions of fibronectin besides the arginine-glycine-aspartic acid sequence required for adhesive function of the cell-binding domain using site-directed mutagenesis. *J. Biol. Chem.* In press.

5. Bodary, S. C., and J. W. McLean. 1990. The integrin beta 1 subunit associates with the vitronectin receptor alpha v subunit to form a novel vitronectin receptor in a human embryonic kidney cell line. *J. Biol. Chem.* 265:5938–5941.
6. Boucaut, J. -C., T. Darribere, T. J. Poole, H. Aoyama, K. M. Yamada, and J. P. Thiery. 1984. Biologically active synthetic peptides as probes of embryonic development: a competitive peptide inhibitor of fibronectin function inhibits gastrulation in amphibian embryos and neural crest cell migration in avian embryos. *J. Cell Biol.* 99:1822–1830.
7. Burnette, W. N. 1981. "Western blotting": electrophoretic transfer of proteins from sodium dodecylsulfate-polyacrylamide gels to unmodified nitrocellulose and radiographic detection with antibody and radiolabeled protein A. *Anal. Biochem.* 112:195–203.
8. Carsons, S. E. 1989. Fibronectin in Health and Disease. CRC Press, Boca Raton, FL. 297 pp.
9. Clark, R. A. F., and P. M. Henson. 1988. The Molecular and Cellular Biology of Wound Repair. Plenum Publishing Corp., NY. 597 pp.
10. Donaldson, D. J., J. T. Mahan, and G. N. Smith. 1987. Newt epidermal cell migration in vitro and in vivo appears to involve Arg-Gly-Asp-Ser receptors. *J. Cell Sci.* 87:525–534.
11. Dufour, S., J. -L. Duband, M. J. Humphries, M. Obara, K. M. Yamada, and J. P. Thiery. 1988. Attachment, spreading and locomotion of avian neural crest cells are mediated by multiple adhesion sites on fibronectin molecules. *EMBO (Eur. Mol. Biol. Organ.) J.* 7:2661–2671.
12. Elices, M. J., L. A. Urry, and M. E. Hemler. 1991. Receptor functions for the integrin VLA-3: fibronectin, collagen, and laminin binding are differentially influenced by ARG-GLY-ASP peptide and divalent cations. *J. Cell Biol.* 112:169–181.
13. Fogerty, F. J., S. K. Akiyama, K. M. Yamada, and D. F. Mosher. 1990. Inhibition of binding of fibronectin to matrix assembly sites by anti-integrin ($\alpha_5\beta_1$) antibodies. *J. Cell Biol.* 111:699–708.
14. Frankel, M. E., and W. Gerhard. 1979. The rapid determination of binding constants for antiviral antibodies by a radioimmunoassay. An analysis of the interaction between hybridoma proteins and influenza virus. *Mol. Immunol.* 16:101–106.
15. Furth, M. E., L. J. Davis, B. Fleurdelys, and E. M. Scolnik. 1982. Monoclonal antibodies to the p21 products of the transforming gene of Harvey murine sarcoma virus and of the cellular *ras* gene family. *J. Virol.* 43:294–304.
16. Giancotti, F., and E. Ruoslahti. 1990. Elevated levels of the $\alpha_5\beta_1$ fibronectin receptor suppress the transformed phenotype of Chinese hamster ovary cells. *Cell.* 60:849–859.
17. Ginsberg, M. H., J. C. Loftus, and E. F. Plow. 1988. Cytoadhesins, integrins, and platelets. *Thromb. Hemostas.* 59:1–6.

17a. Hahn, L. -H. E., and K. M. Yamada. 1979. Isolation and biological characterization of active fragments of the adhesive glycoprotein fibronectin. *Cell.* 18:1043–1051.

18. Hautanen, A., J. Gailit, D. M. Mann, and E. Ruoslahti. 1989. Effects of modifications of the RGD sequence and its context on recognition by the fibronectin receptor. *J. Biol. Chem.* 264:1437–1442.
19. Hayashi, M., and K. M. Yamada. 1983. Domain structure of the carboxyl-terminal half of human plasma fibronectin. *J. Biol. Chem.* 258:3332–3340.
20. Hemler, M. E. 1990. VLA proteins in the integrin family: structures, functions, and their role on leukocytes. *Annu. Rev. Immunol.* 8:365–400.
21. Humphries, M. J., S. K. Akiyama, A. Komoriya, K. Olden, and K. M. Yamada. 1986. Identification of an alternatively-spliced adhesion site in human plasma fibronectin that possesses cell-type specificity. *J. Cell Biol.* 103:2637–2647.
22. Hynes, R. O. 1987. Integrins: a family of cell surface receptors. *Cell.* 48:549–554.
23. Hynes, R. O. 1990. Fibronectins. Springer Verlag, NY. 546 pp.
24. Izzard, C. S., R. Radinsky, and L. A. Culp. 1986. Substratum contacts and cytoskeletal reorganization of BALB/c 3T3 cells on a cell-binding fragment and heparin-binding fragments of plasma fibronectin. *Exp. Cell Res.* 165:320–336.
25. Juliano, R. L. 1987. Membrane receptors for extracellular matrix macromolecules: relationship to cell adhesion and tumor metastasis. *Biochim. Biophys. Acta.* 907:261–278.
26. Katayama, M., F. Hino, Y. Odate, S. Goto, F. Kimizuka, I. Kato, K. Titani, and K. Sekiguchi. 1989. Isolation and characterization of two monoclonal antibodies that recognize remote epitopes on the cell-binding domain of human fibronectin. *Exp. Cell Res.* 185:229–236.
27. Kimizuka, F., Y. Ohdate, Y. Kawase, T. Shimojo, Y. Taguchi, K. Hashino, S. Goto, H. Hashi, I. Kato, K. Sekiguchi, and K. Titani. 1991. Role of type III homology repeats in cell adhesive function within the cell-binding domain of fibronectin. *J. Biol. Chem.* 266:3045–3051.
28. Kornblihtt, A. R., K. Umezawa, K. Vibe-Pedersen, and F. E. Baralle. 1985. Primary structure of human fibronectin: differential splicing may generate at least 10 polypeptides from a single gene. *EMBO (Eur. Mol. Biol. Organ.) J.* 4:1755–1759.
29. Laemmli, U. K. 1970. Cleavage of structural proteins during the assembly

of the head of bacteriophage T4. *Nature (Lond.)*. 227:680–685.
30. Lash, J. W., E. Gosfield, D. Ostrovsky, and R. Bellairs, 1990. Migration of chick blastoderm under the vitelline membrane: the role of fibronectin. *Dev. Biol.* 139:407–416.
31. Lewandowska, K., E. Balza, L. Zardi, and L. A. Culp. 1990. Requirement for two different cell-binding domains in fibronectin for neurite extension of neuronal derivative cells. *J. Cell Sci.* 95:75–83.
32. McCarthy, J. B., A. P. Skubitz, Z. Qi, X. Y. Yi, D. J. Mickelson, D. J. Klein, and L. T. Furcht. 1990. RGD-independent cell adhesion to the carboxy-terminal heparin-binding fragment of fibronectin involves heparin-dependent and -independent activities. *J. Cell Biol.* 110:777–787.
33. MacDonald, J. A. 1988. Extracellular matrix assembly. *Annu. Rev. Cell Biol.* 4:183–207.
34. McDonald, J. A., B. J. Quade, T. J. Broekelman, R. LaChance, K. Forsman, E. Hasegawa, and S. Akiyama. 1987. Fibronectin's cell-adhesive domain and an amino-terminal matrix assembly domain participate in its assembly into fibroblast pericellular matrix. *J. Biol. Chem.* 262:2957–2967.
35. Miekka, S. I., K. C. Ingham, and D. Menache. 1982. Rapid methods for isolation of human plasma fibronectin. *Thromb. Res.* 27:1–14.
36. Mosher, D. F. 1989. Fibronectin. Academic Press, New York. 474 pp.
37. Mugnai, G., K. Lewandowska, B. Carnemolla, L. Zardi, and L. A. Culp. 1988. Modulation of matrix responses of human neuroblastoma cells by neighboring sequences in the fibronectins. *J. Cell Biol.* 106:931–943.
38. Obara, M., M. S. Kang, and K. M. Yamada. 1988. Site-directed mutagenesis of the cell-binding domain of fibronectin: separable, synergistic sites mediate adhesive function. *Cell.* 53:649–657.
39. Pierschbacher, M. D., and E. Ruoslahti. 1984. Cell attachment activity of fibronectin can be duplicated by small synthetic fragments of the molecule. *Nature (Lond.)*. 309:30–33.
40. Pierschbacher, M. D., and E. Ruoslahti. 1984. Variants of the cell recognition site of fibronectin that retain attachment-promoting activity. *Proc. Natl. Acad. Sci. USA.* 81:5985–5988.
41. Pierschbacher, M. D., E. G. Hayman, and E. Ruoslahti. 1981. Location of the cell attachment site in fibronectin with monoclonal antibodies and proteolytic fragments of the molecule. *Cell.* 26:259–267.
42. Roman, J., R. M. LaChance, T. J. Broekelmann, C. J. R. Kennedy, E. A. Wayner, W. G. Carter, and J. A. McDonald. 1989. The fibronectin receptor is organized by extracellular matrix fibronectin: implications for oncogenic transformation and for cell recognition of fibronectin matrices. *J. Cell Biol.* 108:2529–2543.
43. Deleted in proof.
44. Ruoslahti, E., and M. D. Pierschbacher. 1986. Arg-Gly-Asp: a versatile cell recognition signal. *Cell.* 44:517–518.
45. Ruoslahti, E., and M. D. Pierschbacher. 1987. New perspectives in cell adhesion: RGD and integrins. *Science (Wash. DC).* 238:291–297.
46. Ruoslahti, E., E. G. Hayman, E. Engvall, W. C. Cothran, and W. T. Butler. 1981. Alignment of biologically active domains in the fibronectin molecule. *J. Biol. Chem.* 256:7277–7281.
47. Skorstengaard, K., M. S. Jensen, T. E. Petersen, and S. Magnusson. 1986. Purification and complete primary structures of the heparin-, cell, and DNA-binding domains of bovine plasma fibronectin. *Eur. J. Biochem.* 154:15–29.
48. Straus, A. H., W. G. Carter, E. A. Wayner, and S. Hakomori. 1989. Mechanism of fibronectin-mediated cell migration: dependence or independence of cell migration susceptibility on RGDS-directed receptor (integrin). *Exp. Cell Res.* 183:126–139.
49. Streeter, H. B., and D. A. Rees. 1987. Fibroblast adhesion to RGDS shows novel features compared with fibronectin. *J. Cell Biol.* 105:507–515.
50. Varani, J., W. Orr, and P. A. Ward. 1978. Comparison of the migration patterns of normal and malignant cells in two assay systems. *Am. J. Pathol.* 90:159–172.
51. Woods, A., J. R. Couchman, S. Johansson, and M. Hook. 1986. Adhesion and cytoskeletal organisation of fibroblasts in response to fibronectin fragments. *EMBO (Eur. Mol. Biol. Organ.) J.* 5:665–670.
52. Yamada, K. M. 1988. Fibronectin domains and receptors. *In* Fibronectin, D. F. Mosher, editor. Academic Press, New York. 48–121.
53. Yamada, K. M. 1990. Fibronectins: structure, functions and receptors. *Curr. Opin. Cell Biol.* 1:956–963.
54. Yamada, K. M., and D. W. Kennedy. 1984. Dualistic nature of adhesive protein function: fibronectin and its biologically active peptide fragments can autoinhibit fibronectin function. *J. Cell Biol.* 99:29–36.
55. Yamada, K. M., D. W. Kennedy, S. S. Yamada, H. Gralnick, W.-T. Chen, and S. K. Akiyama. 1990. Monoclonal antibody and synthetic peptide inhibitors of human tumor cell migration. *Cancer Res.* 50: 4485–4496.
56. Yokoya, A., K. Kobayashi, Y. Miyamoto, and S. Ishizaka. 1991. Target size for a fibronectin-cell adhesion system determined by the X-ray inactivation method. *Cell Struct. Func.* 16:17–22.
57. Zardi, L., B. Carnemolla, E. Balza, L. Borsi, P. Castellani, M. Rocco, and A. Siri. 1985. Elution of fibronectin proteolytic fragments from a hydroxyapatite chromatography column. A simple procedure for the purification of fibronectin domains. *Eur. J. Biochem.* 146:571–579.